Analogous description of the hydrodynamics of gas–solid fluidized beds and bubble columns

R. Krishna, J. Ellenberger and D.E. Hennephof
Department of Chemical Engineering, University of Amsterdam, Nieuwe Achtergracht 166, NL-1018 WV Amsterdam (Netherlands)

(Received January 15, 1993; in final form May 22, 1993)

Abstract

In this paper we stress analogies in the hydrodynamic behaviour of gas–solid fluidized beds and bubble columns. Using published experimental data, it is demonstrated that the analogous hydrodynamic behaviour is not only qualitative but also quantitative in nature. Specifically, we show the following.

(1) The gas holdup in the homogeneous regimes of bubble columns and fluidized beds can be modelled in a unified way using $V_{slip}=v_{\infty}(1-\epsilon_d)^{n-1}$, where V_{slip} refers to the slip velocity between the dispersed (bubbles or particles) and continuous phases and ϵ_d the dispersed phase holdup. The Richardson–Zaki exponent n decreases with increasing gas density.

(2) The transition from homogeneous to heterogeneous flow regimes in gas–liquid bubble columns and gas–solid fluid beds is delayed by increasing system pressure. Extrapolation of the influence of increased gas density allows us to consider liquid–liquid dispersions and liquid–solid fluid beds as limiting cases.

(3) In the heterogeneous flow regime of operation the classic two-phase theory of fluidized beds can be applied with profit to also describe the hydrodynamics of gas–liquid bubble columns provided that the "dilute" phase is identified with the fast-rising large bubbles and the "dense" phase is identified with the liquid phase containing entrained "small" bubbles. Tentative analogies can also be drawn for the interphase mass transfer processes.

(4) The "dense" phase backmixing can be modelled in a unified manner.

(5) The two-phase theory can be extended to describe slurry reactors.

It is argued that, because of cross-fertilization of concepts and information, appreciation of analogies can be an invaluable tool in scaling up.

1. Introduction

There are several books and reviews dealing with the subject of gas–solid fluidized bed reactors and bubble columns [1–11]. Broadly speaking, the hydrodynamic picture of these two important industrial contactors is as described below.

When a gaseous phase is introduced uniformly through the bottom of a packed bed of particles (see Fig. 1(a)), the bed begins to expand for gas velocities exceeding the minimum fluidization velocity U_{mf}. For fine particles, say smaller than 200 μm, the bed expands uniformly; this is the regime of homogeneous fluidization. This regime of homogeneous fluidization prevails till a certain velocity is reached at which bubbles are first observed; the velocity at this point, U_{mb}, is usually called the minimum bubbling velocity. For the purposes of drawing analogies with gas–liquid systems, we shall denote this velocity as the transition velocity U_{trans}. The operating gas velocity window between U_{mf} and U_{trans} is usually very narrow and it is usually not possible to operate commercial reactors in a stable manner in this regime. On the other hand, in gas–solid beds of large particles, say larger than 1 mm, bubbles appear as soon as the gas velocity exceeds U_{mf} and hence $U_{trans} \approx U_{mf}$. Beyond the gas velocity corresponding to U_{trans} we have the regime of heterogeneous fluidization. In the heterogeneous fluidization regime a small portion of the entering gas is used to keep the solids in suspension while the major portion of the gas flows through the reactor in the form of bubbles. Commercial reactors usually operate in the heterogeneous or bubbling fluidization regime at gas velocities U exceeding 0.1 m s^{-1}, a few orders of magnitude higher than U_{trans}. Under these conditions the bubbles tend to rise up the column very quickly at velocities of the

0923-0467/93/$6.00

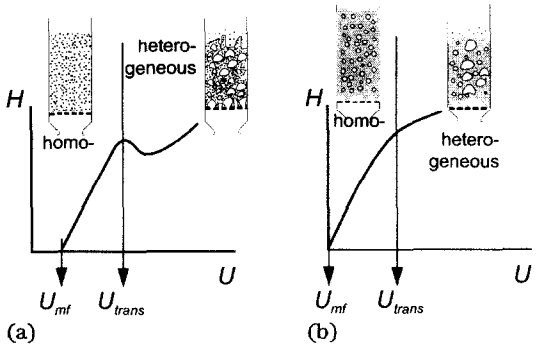

Fig. 1. Homogeneous and heterogeneous flow regimes in (a) gas–solid fluidized beds and (b) gas–liquid bubble columns. U_{mf}, the minimum fluidization velocity, equals zero for bubble columns. The regime transition velocity U_{trans} for a gas–solid fluid bed corresponds to the minimum bubbling velocity U_{mb}.

order of 1 m s^{-1}, "bypassing" the suspended particles. These bubbles tend to churn up the bed, causing the solids phase to be thoroughly backmixed. For highly exothermic reactions, such as regeneration of coked catalyst in fluid catalytic cracking (FCC) regenerators, this backmixing characteristic is desirable from the point of view of thermal equilibration of the reactor contents.

An analogous picture emerges if one sparges gas into a column filled with a liquid (see Fig. 1(b)). The bed of liquid begins to expand as soon as gas is introduced. If we therefore define U_{mf} as the minimum fluidization velocity for a gas–liquid system, we see that $U_{mf}=0$. As the gas velocity is increased beyond the value U_{mf}, the bed of liquid expands homogeneously and the bed height increases almost linearly with the superficial gas velocity. This regime of operation of a bubble column is called the homogeneous bubbly flow regime and is entirely analogous to the regime of homogeneous fluidization for a gas–solid system. The bubble size distribution is narrow and a roughly uniform bubble size in the range 2–7 mm is found. As the gas velocity is increased beyond U_{mf}, the bubble population increases and at a certain gas velocity U_{trans} coalescence of the bubbles takes place to produce the first fast-rising "large" bubbles. The appearance of the first large bubble changes the hydrodynamic picture dramatically. The hydrodynamic picture in a gas–liquid system for velocities exceeding U_{trans} is analogous to the heterogeneous fluidization regime for gas–solid systems and is commonly referred to as the churn-turbulent regime.

The present paper advocates the use of a unified description of the hydrodynamics of bubble columns and fluidized beds; such a unified approach helps to reveal several quantitative hydrodynamic analogies which have potential use in scale-up.

2. Homogeneous flow regime

Consider co-current upflow of two phases in a vertical column, one homogeneously dispersed (d) and the other continuous (c). The slip velocity between the phases is defined as

$$V_{slip}=\left|\frac{U_d}{\epsilon_d}-\frac{U_c}{\epsilon_c}\right|, \qquad \epsilon_d+\epsilon_c=1 \tag{1}$$

where U_d and U_c are the superficial velocities of the dispersed and continuous phases and ϵ_d and ϵ_c are the respective phase holdups. In the homogeneous dispersed flow regime the expansion behaviour is usually modelled using the Richardson and Zaki relationship [12]

$$V_{slip}=v_\infty \epsilon_c^{n-1}=v_\infty(1-\epsilon_d)^{n-1} \tag{2}$$

where v_∞ is the terminal fall (or rise) velocity of a single dispersed "particle", *i.e.* in the limiting case $\epsilon_c \to 1$, $\epsilon_d \to 0$; n is the Richardson–Zaki exponent.

For particulate gas–solid fluidization the dispersed phase can be identified with the particles while the fluidizing gas forms the continuous phase (see Fig. 2(a)). In a laboratory fixed frame of reference there is no net particle flow out of the vertical vessel, *i.e.* $U_d \equiv 0$, and so

$$U_c=v_\infty \epsilon_c^{\,n}=v_\infty(1-\epsilon_d)^n \tag{3}$$

where U_c is the superficial gas velocity and ϵ_c is the bed voidage. For drawing analogies with gas–liquid bubble columns it is convenient to define the parameter $V_{slip}\epsilon_c$, which for gas–solid fluid beds reduces to

$$V_{slip}\epsilon_c \equiv U_c=v_\infty \epsilon_c^{\,n} \tag{4}$$

The expressions (3) and (4) have been used with success to correlate fluid bed expansion behaviour. Figure 3(a) shows typical data for fluidization of FCC with helium as fluidizing gas [13]. Extrapolation of the data in the homogeneous fluidization regime to $\epsilon_c=1$ yields the value of v_∞ while the slope of the log–log plot of U_c *vs.* ϵ_c yields the Richardson–Zaki exponent n. The Richardson–Zaki n generally decreases with increasing gas density, as seen in Fig. 4(a) for particulate expansion of FCC [13] and carbon powders [14]. For relatively large particles of glass ballotini, $d_p=175$ μm, the Richardson–Zaki index is practically independent of the gas density [17]. For all particle sizes the single-particle terminal velocity v_∞ decreases with increasing gas density (see Fig. 5(a)).

For gas–liquid bubble columns with no net liquid flow, *i.e.* $U_c \equiv 0$ (Fig. 2(b)), eqns. (1) and (2) simplify

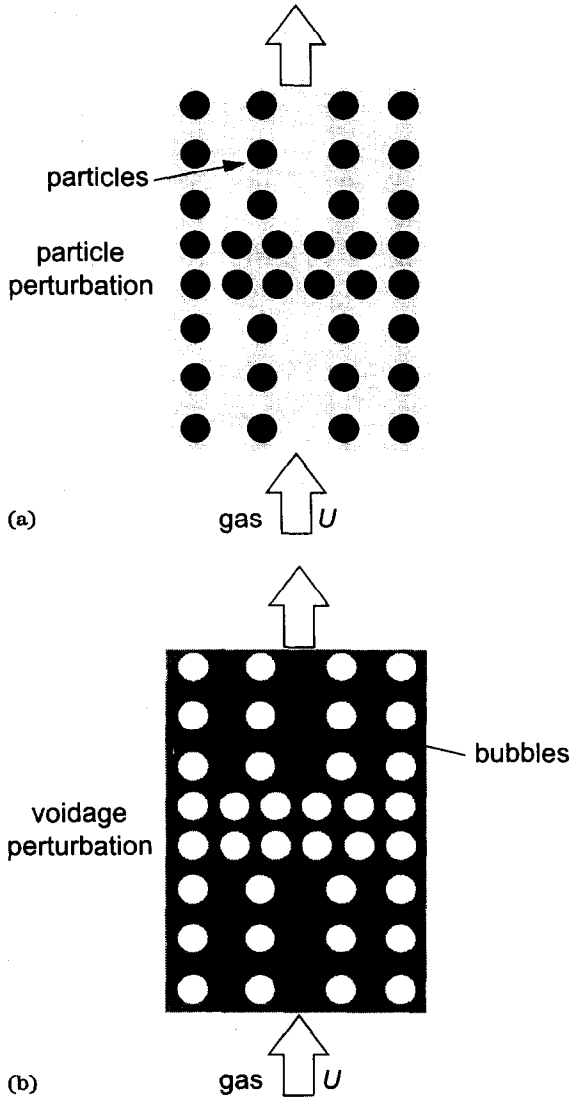

Fig. 2. Homogeneous flow in dispersed two-phase flow in vertical columns. The figure also shows perturbations of dispersed phase holdups in (a) gas–solid fluid beds and (b) bubble columns.

to yield

$$V_{slip} \equiv \frac{U_d}{\epsilon_d} = v_\infty (1-\epsilon_d)^{n-1} \tag{5}$$

where V_{slip} now corresponds to the (absolute) rise velocity of the bubble swarm. The parameter $V_{slip}\epsilon_c$ is thus

$$V_{slip}\epsilon_c \equiv \frac{U_d(1-\epsilon_d)}{\epsilon_d} = v_\infty (1-\epsilon_d)^n \tag{6}$$

which is analogous to eqn. (4). Some typical experimental data are illustrated in Fig. 3(b) for air–tetradecane [15]. From the slope of the log–log plot in Fig. 3(b) the Richardson–Zaki exponent n can be determined. For liquids with relatively low viscosity, such as water, the Richardson–Zaki index

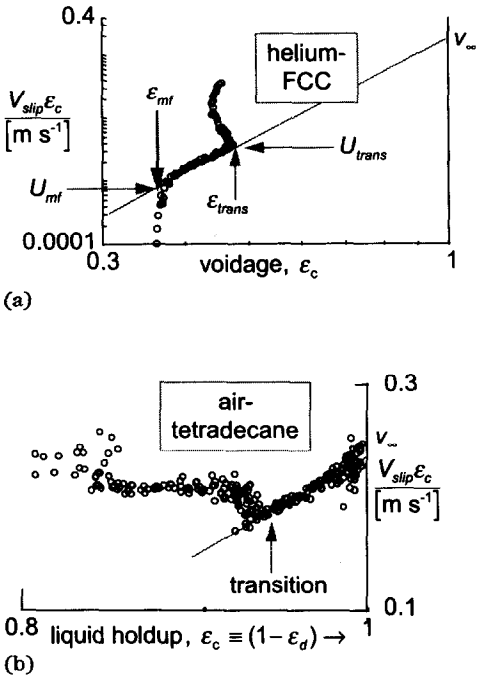

Fig. 3. (a) Log–log plot of typical experimental data of $V_{slip}\epsilon_c$ ($\equiv U_c$) *vs.* bed voidage ϵ_c for the system helium–FCC. Data from Ellenberger and Kouwenhoven [13] obtained in a column 0.1 m in diameter. (b) Log–log plot of typical experimental data for $V_{slip}\epsilon_c$ as a function of $1-\epsilon_d$, where ϵ_d is the gas holdup. Measurements made by Hennephof [15] in a column 0.1 m in diameter with tetradecane as the liquid phase and air as the gas phase. The transition to the heterogeneous flow regime is characterized in both plots (a) and (b) by a departure from linearity on the log–log plot. The intercept on the $\epsilon_c = 1$ axis corresponds to the single-particle (bubble) rise velocity v_∞.

n shows a pronounced decreases with increasing gas density (see Fig. 4(b)). With tetradecane as the liquid phase ($\rho_L = 753$ kg m^{-3}, $\mu_L = 2.2$ mPa s) the Richardson–Zaki index is practically constant; this is in analogy with the behaviour of large glass ballotini particles with $d_p = 175$ μm. Broadly speaking, the behaviour of larger particles is analogous to that of more viscous liquids.

Figure 5(b) shows the variation in the single-bubble rise velocity v_∞ for gas–liquid systems as a function of the gas density. Generally speaking, the single-bubble rise velocity decreases with increasing gas density, but this decrease is less pronounced than that exhibited by gas–solid systems (compare Figs. 5(a) and 5(b)).

2.1. Transition from homogeneous to heterogeneous flow regime

For fine powders the particulate or homogeneous fluidization regime persists till a certain gas velocity called the minimum bubbling point U_{mb} ($= U_{trans}$) is reached, whereupon transition takes place to the

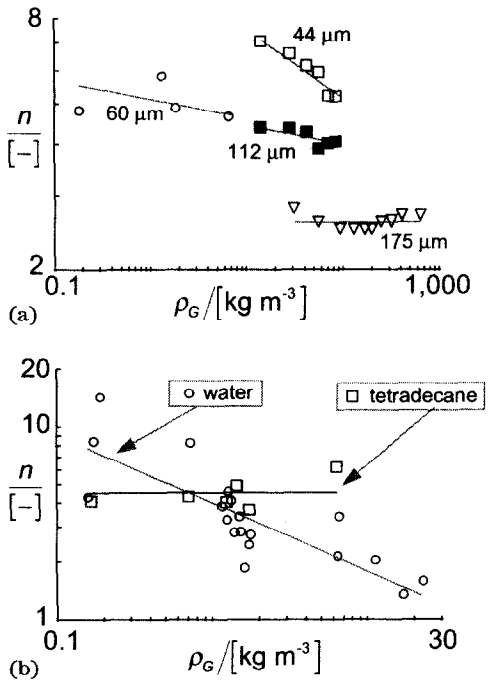

Fig. 4. (a) The Richardson–Zaki index n for homogeneous fluidization of FCC, fine carbon powders and glass ballotini as a function of the density of the fluidizing gas. Data for FCC ($d_p = 60$ μm) from Ellenberger and Kouwenhoven [13] obtained in a column 0.1 m in diameter. Data for activated carbon powders ($d_p = 44$ and 112 μm) from Jacob and Weimer [14]. Data for glass ballotini ($d_p = 175$ μm) from Poletto *et al.* [17]. (b) The Richardson–Zaki index as a function of the gas density for bubble columns with water and tetradecane as the liquid phases. Water data from Krishna *et al.* [16]. Tetradecane data from Hennephof [15].

heterogeneous flow regime. The transition gas velocity is very sensitive to particle size, particle size distribution and the system pressure [13, 14, 17, 18]. Let us now focus on the influence of the density of the fluidizing gas on the regime transition velocity.

The experimental data in Fig. 6(a) show that increasing the gas density tends to increase the range of homogeneous fluidization — witness the increase in $\epsilon_{trans} - \epsilon_{mf}$ with increasing gas density. From Fig. 6(a) it can be seen that the window of particulate expansion, $\epsilon_{trans} - \epsilon_{mf}$, decreases when the particle size increases.

Analogous to the behaviour of gas–solid fluid beds observed above, an increase in gas density tends to delay the transition from the homogeneous to the heterogeneous flow regime in bubble columns [15, 16]. Figure 6(b) shows the data for ϵ_{trans} for systems with water and tetradecane as the liquid phase. For the more viscous liquid tetradecane the window of operation of homogeneous bubbly flow is narrower than that for water; this is analogous to the observation made earlier on the behaviour of particles of large diameter. Viewed another way, Figs. 6(a) and 6(b) provide further evidence of the equivalence of the behaviour of large particles and viscous liquids.

The delaying effect of the gas density on the flow regime transition point in fluid beds and bubble columns can be understood physically by means of Fig. 2. Let us take the specific example of a bubble column to start with (Fig. 2(b)) and introduce a perturbation of voidage by means of a horizontal slice of bubble dispersion with a greater voidage than in the surrounding region. From eqn. (5) it follows that the slip velocity of the bubble swarm in the perturbed region of higher voidage is lower than the slip velocity of the dispersion around it. This will cause the bubble swarm below the perturbation to "catch up" with the perturbed bubble swarm and therefore there will be a tendency for bubble movement from a lower voidage region to a region of higher voidage. This destabilizing force is proportional to the variation in $V_{slip}\epsilon_c$ with voidage:

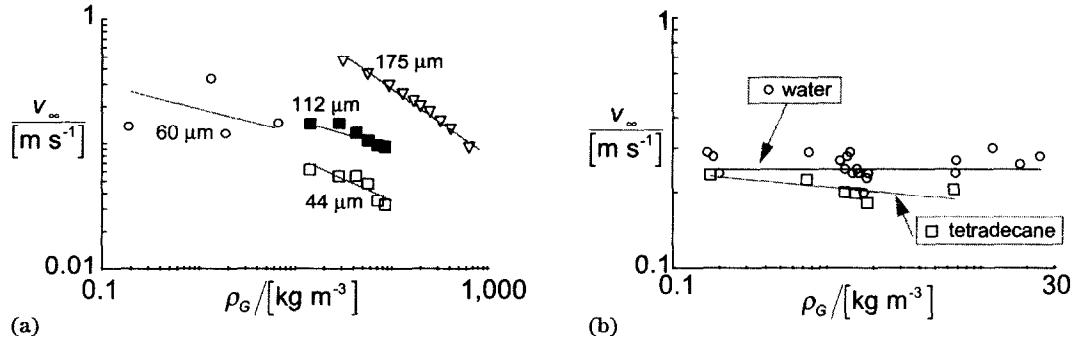

Fig. 5. (a) The terminal velocity v_∞ for homogeneous fluidization of FCC, fine carbon powders and glass ballotini as a function of the density of the fluidizing gas. Data sources as in caption to Fig. 4. (b) The single-bubble rise velocity v_∞ as a function of the gas density for bubble columns with water and tetradecane as the liquid phases. Data sources as in caption to Fig. 4.

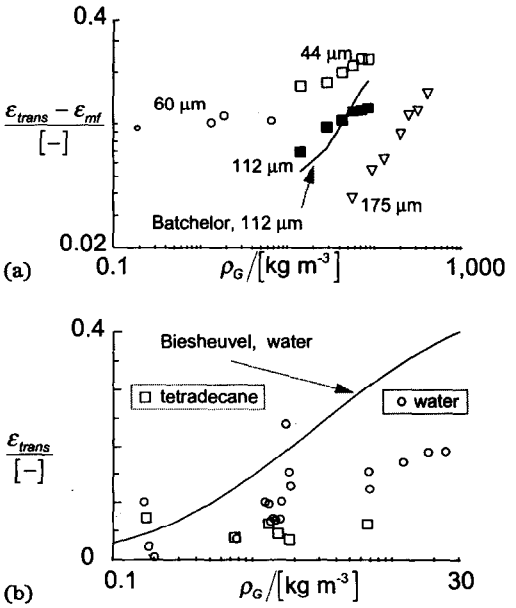

Fig. 6. (a) Variation in $\epsilon_{trans}-\epsilon_{mf}$ for FCC, carbon powders and glass ballotini as a function of the gas density. Data sources as in caption to Fig. 4. The Batchelor stability analysis for carbon powder with $d_p=112$ μm is also indicated. (b) The gas holdup at the regime transition point, ϵ_{trans} as a function of the gas density for bubble column operation with water and tetradecane as the liquid phases. Data sources as in caption to Fig. 4. The continuous curve corresponds to the application of the Biesheuvel–Gorissen stability analysis for water [16, 19, 20].

$$\text{destabilizing force } \alpha \frac{\partial(V_{slip}\epsilon_c)}{\partial\epsilon_d} \alpha$$

$$v_\infty \frac{\partial(1-\epsilon_d)^n}{\partial\epsilon_d} = nv_\infty(1-\epsilon_d)^{n-1} \tag{7}$$

Countering this destabilizing force are two types of force: (i) the force generated by random bubble motions tending to smear out voidage fluctuations and (ii) the force arising from dispersion (or diffusion) of the voidage perturbation from high voidage to lower voidage. From eqn. (7) it should be clear that if $n=0$, there is no destabilizing force. A larger value of n signifies a large destabilizing influence. An increase in the gas density in bubble columns leads to a decrease in the value of the product nv_∞ (see Figs. 4(b) and 5(b)) and consequently a reduced probability of propagation of instabilities, leading to delayed flow regime transition (see Fig. 6(b)). With water as the liquid phase the reduction in nv_∞ with increasing gas density ρ_G is more pronounced than with viscous tetradecane (cf. Figs. 4(b) and 5(b)) and consequently for water an increase in ρ_G has a greater increasing effect on ϵ_{trans} than for tetradecane.

The stability analysis discussed above forms the basis of the approach of Biesheuvel and Gorissen [19]. Krishna and coworkers [16, 20] have modified the Biesheuvel–Gorissen analysis to include the influence of gas density on the Richardson–Zaki exponent n. The results of their calculations for ϵ_{trans} for water are shown in Fig. 6(b) as a continuous curve and it may be noted that the experimentally observed transition data for water lie predominantly below the stability boundary.

For gas–solid fluid beds a comprehensive stability analysis similar to the Biesheuvel–Gorissen analysis has been presented by Batchelor [21] in an authoritative paper. From Figs. 4(a) and 5(a) we note that the product nv_∞ decreases with increasing gas density for fluid beds. This implies that the destabilizing force decreases with increasing gas density. This provides a qualitative explanation for the observed stabilizing influence of increased gas density (see Fig. 6(a)). Some of the parameters in the Batchelor analysis are only given as order-of-magnitude estimates. Nevertheless, using measured and assumed parameters values, we carried out calculations of $\epsilon_{trans}-\epsilon_{mf}$ for the set of measurements for carbon powder with $d_p=112$ μm reported by Jacob and Weimer [14]. The results of the Batchelor analysis for the six data points are depicted as a continuous curve. It can be seen that the Batchelor analysis is able to essentially reproduce the observed influence of gas density in delaying the flow regime transition.

From a hydrodynamic viewpoint a liquid phase can be considered as being the limiting case of increased gas density (see Fig. 7). For liquid–liquid spray columns it is usual to choose $n=2$, *i.e.*

$$V_{slip}=v_\infty(1-\epsilon_d), \qquad V_{slip}\epsilon_c=v_\infty(1-\epsilon_d)^2 \tag{8}$$

but experiments show a range of values of n varying from 1.5 to 2 [22]. Liquid–liquid spray columns usually operate in the homogeneous regime and flooding takes place before transition to the heterogeneous regime can be realized, as illustrated in the calculations of Fig. 8.

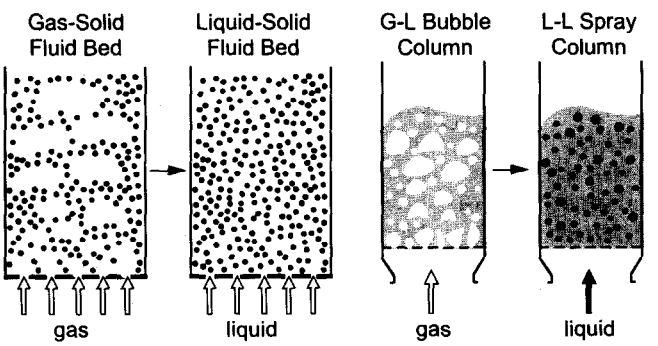

Fig. 7. Limiting cases of gas–solid fluid beds and bubble columns obtained with increasing gas density.

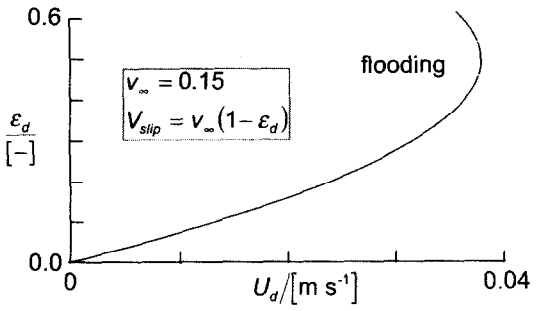

Fig. 8. Calculation of the dispersed phase holdup for a liquid–liquid spray column as a function of the dispersed phase superficial velocity. The curve is drawn with the single-bubble rise velocity $v_\infty = 0.15$ m s^{-1}, taking the Richardson–Zaki index $n = 2$.

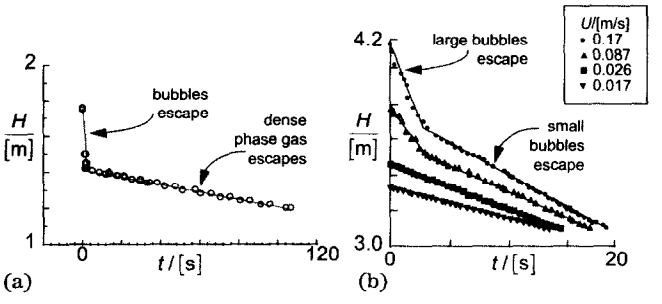

Fig. 9. Typical bed collapse experiments for gas–solid fluid beds and gas–liquid bubble columns. (a) Bed collapse data for FCC powder in a column 0.38 m in diameter operating at a superficial gas velocity of 0.282 m s^{-1}. Data from Ellenberger and Kouwenhoven [13]. (b) Bed collapse experiments in a gas–liquid bubble column with methanol as the liquid phase. Data from Schumpe and Grund [24] and Grund [25].

A liquid–solid fluidized bed, which can be considered as a limiting case of a gas–solid fluid bed (see Fig. 7), operates predominantly in the homogeneous regime and transition to the heterogeneous flow regime takes place for large ratios ρ_p/ρ_L [3, 23].

3. Heterogeneous flow regime

Let us perform a bed collapse experiment in the heterogeneous flow regime; in this experiment the gas supply is instantaneously shut off and the height–time information is recorded continuously. Figure 9(a) is typical of bed collapse experiments with gas–solid fluid beds. The initial sharp decrease in height is due to the escape of bubbles; this is followed by slow disengagement of the gas entrapped in the dense phase. Figure 9(b) represents analogous bed collapse experiments in a gas–liquid bubble column. For gas velocities below U_{trans} we have homogeneous bubbly flow and in this regime the disengagement curve follows a linear path (in the experiments shown in Fig. 9(b) this regime prevails for $U < 0.026$ m s^{-1}). For superficial gas velocities exceeding U_{trans} the bed collapse shows two distinct regimes. Initially we have disengagement of the fast-rising large bubbles and this is followed by disengagement of the small bubbles. In the experiments portrayed in Fig. 9(b) the heterogeneous flow regime prevails at velocities $U > 0.087$ m s^{-1}. A bimodal size distribution is suggested by the disengagement curves in Fig. 9(b); such bimodal distributions have been confirmed by several workers [4, 5, 25–27]. The bed collapse curves for fluid beds and bubble columns are analogous.

On the basis of the bed collapse experiments, we can determine for fluid beds and bubble columns the bed expansion ϵ^{exp} and the total gas holdup ϵ_{total} respectively:

$$\epsilon^{exp} = \frac{H - H_0}{H_0}, \qquad \epsilon_{total} = \frac{H - H_0}{H} \tag{9}$$

where H_0 is the height of the ungassed bed. Figure 10(a) shows some typical fluid bed expansion data. The dense phase gas expansion is seen to be practically constant; the gas velocity in excess of that required to keep the dense phase in suspension is transported in the form of fast-rising bubbles.

An analogous picture emerges for a bubble column. Some typical holdup data are shown in Fig. 10(b) for the system air–methanol [5, 24, 25]. In the heterogeneous regime the holdup of the small bubbles is practically constant. The small bubbles can be considered to be entirely analogous to the dense phase gas in a gas–solid fluid bed. The superficial gas velocity through the dense phase in either bubble columns or fluid beds is approximately equal to the gas velocity at the regime transition point, *i.e.* $U_{df} \approx U_{trans}$. The superficial gas velocity in excess of U_{df} moves up the column as fast-rising large bubbles. For both fluid beds and bubble col-

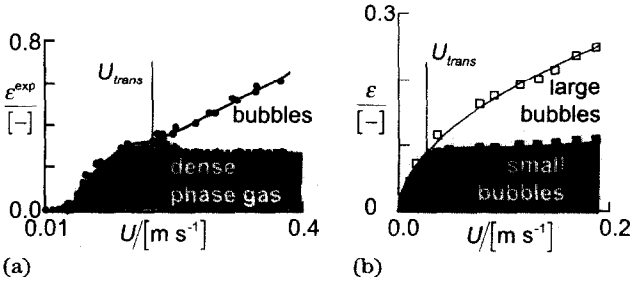

Fig. 10. (a) Typical bed expansion $\epsilon^{exp} \equiv (H - H_0)/H_0$ *vs.* superficial gas velocity data for a fluid bed with porous chalk-like limestone as the solids phase. Data from Roes and Garnier [26]. (b) Total gas holdup ϵ_{total} and small bubble gas holdup ϵ_{small} in a bubble column with methanol as the liquid phase. Data from Grund [25].

umns the regime transition point U_{df} increases significantly with increasing gas density (*i.e.* pressure); this fact has a significant consequence for mass transfer from the fast-rising bubbles, considered in the next section.

Figure 11 shows values of the rise velocities for fluid beds and bubble columns. The bubble rise velocities in gas–solid fluid beds are of the same order of magnitude as the rise velocities of the large bubble population in gas–liquid systems. In order to stress the analogy, we use the same nomenclature V_{large} for the two cases. The bubble rise velocities in gas–solid fluid beds are known to be scale dependent [28]; bubbles of the same size rise faster in columns of larger diameter than in columns of smaller diameter (see Fig. 12(a)). It is only very recently that experimental data from gas–liquid bubble columns have revealed a scale dependence of the large bubble rise velocity (see Fig. 12(b)) [24, 25, 29]. The results presented in Fig. 12(b) need to be verified further because of their important consequences for scale-up.

On the basis of the hydrodynamic picture emerging above, we may extend the classical two-phase model for fluid beds [30] to bubble columns; this is shown in Fig. 13. The two phases are to be identified as follows.

(1) The "dilute" phase relates to the solids-free bubbles in a fluid bed or the fast-rising large bubble population in bubble columns. The dilute phase travels up the column in plug flow.

(2) The "dense" phase in a fluid bed consists of the suspension of solids with a gas flow corresponding to U_{df}. For bubble columns the dense phase is to be identified with the liquid phase together with the small bubbles which are entrained in the liquid. In the heterogeneous flow regime the small bubbles have the backmixing characteristics of the liquid phase. In columns of large diameter the dense phase can be considered to be completely backmixed.

For a proper modelling of bubble holdups and interphase mass transfer in gas–solid fluid beds, the phenomenon of bubble growth in the region above the distributor needs to be taken into account [3, 7]. A simple physical picture of bubble growth due to coalescence was suggested by Darton *et al.* [31] and is pictured in Fig. 14. In this model coalescence occurs between bubbles of neighbouring streams and the distance travelled by the bubbles before coalescence is considered to be proportional to their horizontal separation from neighbouring bubbles. Darton *et al.*'s model yields the following expression for the bubble diameter as a function of the height above the distributor, h:

$$d \propto (U - U_{df})^{2/5}(H + h_0)^{4/5} \tag{10}$$

The parameter h_0 characterizes the distributor and specifies the initial bubble size formed here. The bubble growth in gas–solid fluid beds does not proceed indefinitely and for fine particles this growth is limited to a maximum stable equilibrium size d^* reached at some distance h^* above the distributor:

$$d^* \propto (U - U_{df})^{2/5}(h^* + h_0)^{4/5}, \qquad h \leqslant h^* \tag{11}$$

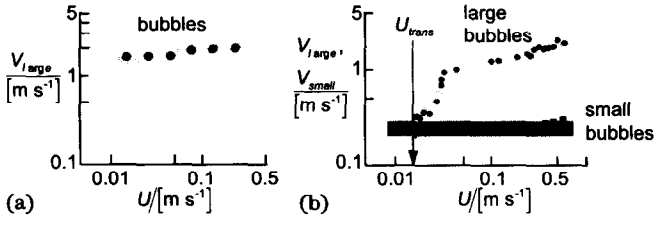

Fig. 11. (a) Typical rise velocities of bubbles in a fluid bed with porous chalk-like limestone as the solids phase. Data from Roes and Garnier [26]. (b) Rise velocities of large and small bubbles in an air–water bubble column. Data from Wezorke [27].

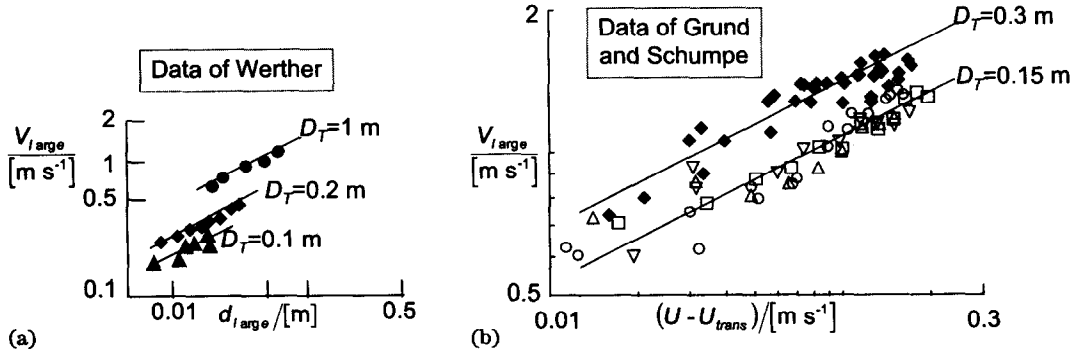

Fig. 12. (a) Influence of column diameter D_T on the rise velocities in gas–solid fluid beds. Data from Werther [28]. (b) Influence of column diameter on the rise velocities in gas–liquid bubble columns. Data from Grund and coworkers [24, 25, 29].

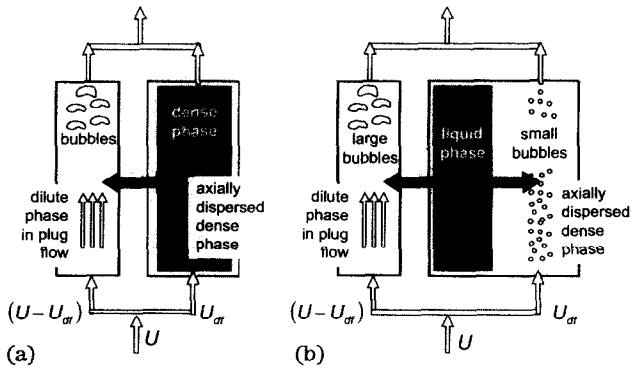

Fig. 13. (a) Classical two-phase model for gas–solid fluid beds, after van Deemter [30]. (b) Extension of two-phase model to bubble columns. The two-headed arrows represent the interphase mass transfer processes.

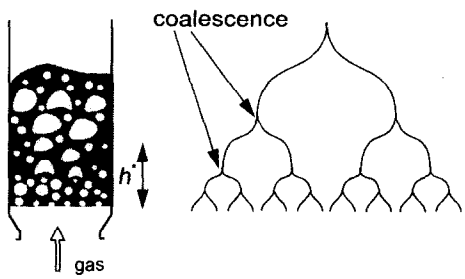

Fig. 14. Darton *et al.'s* model for bubble growth in a gas–solid fluid bed [31].

The equilibrium bubble size d^* is a function of particle size, particle size distribution, the system pressure and physical properties of the fluidizing gas [7]. For Geldart A-type powders d^* has values in the range 0.05–0.3 m. The corresponding values of h^* are in the range 0.5–2 m [26].

The (local) bubble rise velocity in a fluid bed is proportional to the square root of the bubble diameter and the consequence of eqns. (10) and (11) is that the average bubble rise velocity U_{large} for a finite bed height should depend on the height of the expanded bed, H. The average bubble holdup is [32–34]

$$\epsilon_{\text{large}} \propto \frac{1}{H}\int_0^H \frac{U-U_{\text{df}}}{(gd)^{1/2}}\,\mathrm{d}h \tag{12}$$

Insertion of eqns. (10) and (11) into eqn. (12) yields the following dependence of the average bubble holdup on the velocity of gas flowing through the dilute phase, $U-U_{\text{df}}$:

$$\epsilon_{\text{large}} \propto (U-U_{\text{df}})^{4/5} \tag{13}$$

Experimental results of the bubble holdup obtained for FCC powder [32–34] confirm the four-fifths power dependence anticipated by eqn. (12); the results are shown in Fig. 15(a).

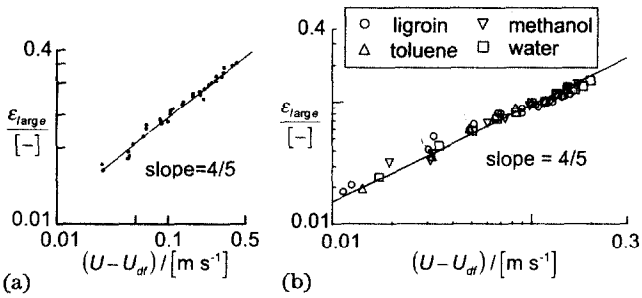

Fig. 15. (a) Measured bubble holdup in a gas–solid fluid bed with FCC powder [32–34] as a function of $U-U_{\text{df}}$. (b) Large bubble holdup in bubble columns with water, methanol, toluene and ligroin as the liquid phases [24, 25]. For the calculations here we used the constant values for U_{df} as follows: water, 0.015; methanol, 0.017; toluene, 0.020; ligroin, 0.02 m s^{-1}.

For bubble columns the equilibrium large bubble size is about 0.05–0.08 m and this stable size is reached in a zone about 0.1–0.3 m above the distributor. The large bubbles may be considered to be formed as a result of the coalescence of small bubbles. If we accept the Darton *et al.* coalescence model to describe the growth of small bubbles to reach the stable equilibrium bubble size d^*, we should expect eqns. (10) and (11) to hold for bubble columns. Above the equilibration height h^* the large and small bubble populations coexist in dynamic equilibrium. Further, the large bubble rise velocity should also be expected to be proportional to $(gd^{1/2})$ as for Taylor bubbles [11]. The above reasoning would lead us to conclude the applicability of eqns. (12) and (13) to bubble columns. We checked this expectation using the large bubble holdup data of Grund [25]; the results are shown in Fig. 15(b). The four-fifths power dependence of ϵ_{large} on $U-U_{\text{df}}$ appears to be confirmed – another analogy with gas–solid fluid beds. It is further remarkable to note that the large bubble holdup is virtually independent of the liquid phase properties. The data of Krishna *et al.* [18] have shown that the large bubble holdup is independent of the gas density.

4. Mass transfer from dilute to dense phase

In the heterogeneous flow regime the interphase mass transfer between the dilute and dense phases is important in determining the reactor conversion. For gas–solid fluid beds with fine particles the mass transfer from bubbles is by two mechanisms, convection (through-flow) and diffusion. The through-flow contribution is usually dominant for fine particles (see Fig. 16(a)). If we accept the model of Davidson *et al.* [11] to describe the interphase mass

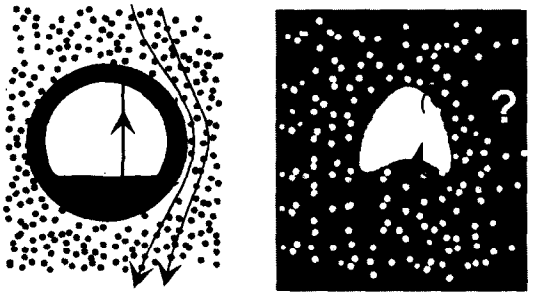

Fig. 16. Through-flow mass transfer from dilute to dense phases. (a) Bubble dense phase mass transfer. (b) Exchange between large and small bubbles?

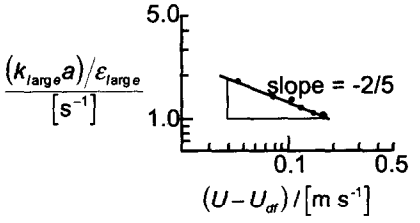

Fig. 17. Mass transfer from the dilute phase to the dense phase for fluid beds of sand. Data from Krishna [34].

transfer process, we find that the mass transfer per unit volume of dispersed bubbles is

$$\frac{k_{large}a}{\epsilon_{large}} \propto \frac{U_{df}}{d} \tag{14}$$

Combining eqn. (13) with eqn. (10) leads to the relation

$$\frac{k_{large}a}{\epsilon_{large}} \propto U_{df}(U-U_{df})^{-2/5} \tag{15}$$

The $-2/5$ power dependence on $U-U_{df}$ has been confirmed by Krishna [34] for fluidized beds of sand; his results are shown in Fig. 17.

Although mass transfer in bubble columns has been studied extensively [4, 5], there are few data on mass transfer from large bubbles. Vermeer and Krishna [35] have reported measurements for mass transfer from large bubbles and attributed the unexpectedly high mass transfer coefficient to a much higher degree of turbulence in the liquid phase surrounding these bubbles. In the light of the analogy arguments presented in this paper, we may wonder if there is a mechanism for mass transfer from large bubbles equivalent to through-flow in fluid beds (see Fig. 16(b)). This through-flow mechanism could involve the exchange of gas between large and small bubbles, a much more effective mass transfer mechanism than molecular diffusion. Small bubbles could be entrained into the wake of large bubbles and get sheared off at the top, resulting in a convective contribution. If this conjecture is true, we should expect the mass transfer from large bubbles to follow the trend predicted by eqn. (15). This aspect needs to be checked experimentally.

5. Dense phase backmixing

In the heterogeneous flow regime the fast-rising large bubbles tend to concentrate towards the centre of the column and entrain solids (fluid beds) or liquid (bubble columns) along with them. When the large bubbles disengage at the top, the entrained solids or liquid flow down the walls [36]. Typical velocity profiles in the dense phase are shown in Fig. 18. The mechanism causing backmixing of the dense phase in fluid beds and bubble columns is thus the same. Further, since the rise velocities of the dilute phase are comparable in the two cases (see Fig. 11), we should expect the dense phase axial dispersion coefficients for fluid beds and bubble columns to have similar numerical values. This has indeed been confirmed experimentally by Baird and Rice [37], who suggested the following empirical correlation for the dense phase axial dispersion coefficient:

$$D_{ax} = 0.35(gU)^{1/3}(D_T)^{4/3} \tag{16}$$

where D_T is the reactor tower diameter. The correlation (16) was found to be applicable also to liquid–liquid systems, which represent the limiting case of gas–liquid systems (see Fig. 7).

6. Slurry reactors

In slurry reactors fine solids (typically smaller than about 200 μm) are suspended in the liquid

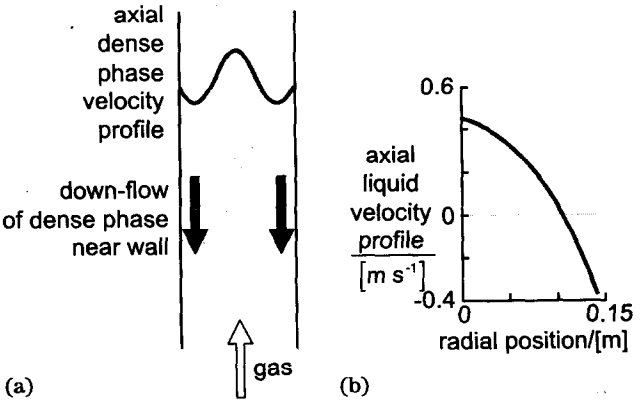

Fig. 18. (a) Axial dense phase velocity profile. (b) Experimentally measured axial liquid velocity profile for bubble columns [36].

phase; these solids are either catalyst particles, reactant or product. One important process for the future using this type of reactor is the slurry phase Fischer–Tropsch synthesis of middle distillate from syngas ($CO + H_2$). As in the case of bubble columns, such sparged slurry reactors are usually operated at superficial gas velocities in the range 0.02–0.3 m s^{-1}. Since the solids are very fine, these would be intimately mixed with the liquid. In tall, narrow laboratory reactors there could well be a solids concentration gradient along the length of the reactor [38], but in large diameter industrial columns, owing to a much higher degree of mixing, the solids phase would tend to be almost well mixed. In fact, for exothermic catalysed reactions such as the Fischer–Tropsch synthesis it is undesirable to have a solids concentration gradient. To prevent solids settling, it is essential to have a small upward movement of the liquid phase co-current with the gas phase. For design and scale-up purposes the slurry phase can be considered as a single entity "moving" together. This tends to simplify the hydrodynamic picture considerably and we may therefore use the physical models developed earlier for gas–liquid bubble columns. Figure 19 shows the extension of the two-phase fluid model to a three-phase slurry reactor.

The influence of the catalyst particles on the hydrodynamics can be expected to be quite complex. Firstly, the presence of the solid particles would enhance the "apparent" viscosity of the liquid. Secondly and more seriously, the presence of the solid particles would affect the coalescence–break-up processes, especially when two small bubbles collide with each other. We should expect the precise effect of the solid particles to depend on their size. For example, particles of a size of say 5–10 μm may not be capable of breaking up the film between two colliding small bubbles. On the other hand, particles of size 50–200 μm could well break up the intervening film and thus promote coalescence

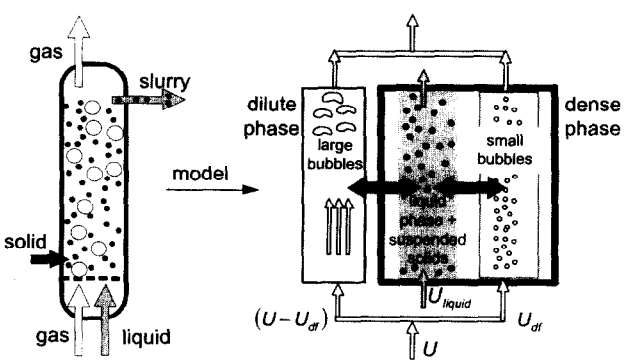

Fig. 19. Two-phase model for a three-phase slurry reactor.

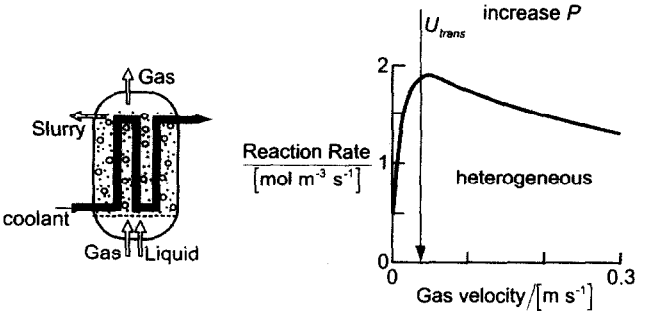

Fig. 20. Simulations for a Fischer–Tropsch slurry reactor using the two-phase model shown in Fig. 19. Adapted from Krishna [34].

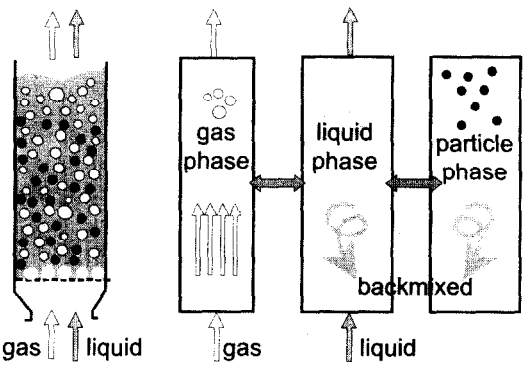

Fig. 21. Model for a three-phase fluidized bed.

of the small bubbles. We should therefore expect the small bubble holdup to be reduced in a slurry reactor when compared with a gas–liquid bubble column. Careful, controlled experimentation is required to determine the influence of solids, with increasing concentration, on the small and large bubble holdups in a slurry reactor. Intuitively we should not expect the large bubble population to be affected to any great extent. One experimental study of the influence of solid particles on bubble hydrodynamics is by Khare and Joshi [39].

The two-phase model for a slurry reactor (Fig. 19) has been applied to the simulation of the Fischer–Tropsch slurry reactor [34]; the results are shown in Fig. 20. The reaction rate displays a maximum at the regime transition point and decreases as the operation progresses into the heterogeneous flow regime. This underlines the importance of predicting the regime transition velocity U_{trans}. The influence of the system operating pressure on the regime transition velocity is also of paramount importance in determining the reactor performance.

7. Three-phase fluidized beds

The terminology three-phase fluidized bed or ebullated bed is usually used for reactors in which the

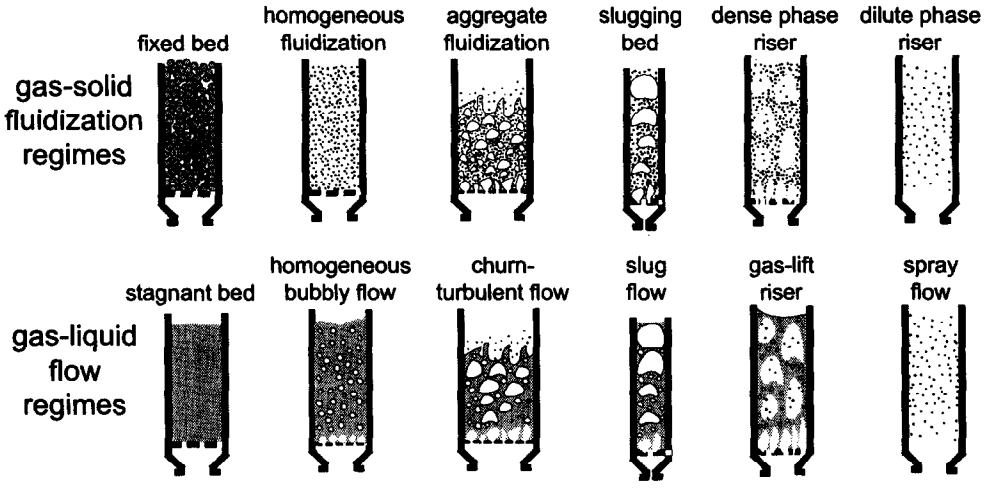

Fig. 22. Flow regime map for two-phase flow in vertical columns.

solid particles are larger than 1 mm. The particles are fluidized by the liquid phase and there is usually a solids-free "freeboard" at the top of the bed (see Fig. 21). The solid particles generally tend to promote bubble break-up and the magnitude of this effect depends on the particle size and particle holdup [6, 40, 41]. The mixing characteristics of the solids phase may be quite distinct from that of the liquid phase and the appropriate physical model to consider is shown in Fig. 21. It remains an intellectual challenge to extend the hydrodynamic analogies discussed in this paper to cover three-phase fluidized beds.

8. Concluding remarks

In this paper we have stressed various hydrodynamic analogies in the operation of gas–solid fluidized beds and gas–liquid bubble columns. If we consider the complete flow regime map for gas–solid and gas–liquid systems in vertical columns, we notice a one-to-one correspondence (see Fig. 22). The analogies between slugging gas–solid and gas–liquid systems have been emphasized by Davidson *et al.* [11]. Turbulent fluid beds and circulating fluid bed risers are gaining importance for exothermic reactions [42]. The hydrodynamics of three contactors is complicated [43] and there may be advantages in seeking analogies with the gas lift reactors which are highly popular in biotechnology [44]. The analogous approach needs to be extended to include liquid–liquid and liquid–liquid–solid systems.

At several points during the discussion we have stressed the need to make a proper distinction between flow regimes. There is a need to better understand flow regime transitions and the development of a unified theory of multiphase flow regime transitions will be useful and enlightening. The appreciation of these analogies allows a unified approach to design and scale-up. Cross-fertilization of design information is possible by employing an analogous approach; this leads to savings in reactor development costs.

References

1 A. Bisio and R.L. Kabel (eds.), *Scaleup of Chemical Processes*, Wiley, New York, 1985.
2 J.J. Carberry and A. Varma (eds.), *Chemical Reaction and Reactor Engineering*, Marcel Dekker, New York, 1987.
3 J.F. Davidson, R. Clift and D.F. Harrison (eds.), *Fluidization*, Academic, New York, 2nd edn., 1985.
4 W.-D. Deckwer, *Bubble Column Reactors*, Wiley, New York, 1992.
5 W.-D. Deckwer and A. Schumpe, Improved tools for bubble column reactor design and scale-up, *Chem. Eng. Sci.*, *48* (1993) 889–911.
6 L.S. Fan, *Gas–Liquid–Solid Fluidization Engineering*, Butterworths, Boston, MA, 1989.
7 D. Geldart (eds.), *Gas Fluidization Technology*, Wiley, New York, 1986.
8 D. Kunii and O. Levenspiel, *Fluidization Engineering*, Butterworth–Heinemann, Boston, MA, 2nd edn., 1991.
9 H.I. de Lasa (ed.), *NATO Advanced Study Institute Series*, No. 110, *Chemical Reactor Design and Technology*, Martinus Nijhoff, Dordrecht, 1986.
10 T. Miyauchi, S. Furusaki, S. Morooka and Y. Ikada, Transport phenomena and reaction in fluidized catalyst beds, *Adv. Chem. Eng.*, *11* (1981) 275–448.
11 J.F. Davidson, D. Harrison, R.C. Darton and R.D. LaNauze, The two-phase theory of fluidization and its application to chemical reactors, in L. Lapidus and N.R. Amundson (eds.), *Chemical Reactor Theory, a Review*, Prentice-Hall, Englewood Cliffs, NJ, 1977, pp. 583–685.

12 J.F. Richardson and W.N. Zaki, Sedimentation and fluidization: Part I, *Trans. Inst. Chem. Eng., 32* (1954) 35–53.
13 J. Ellenberger and P. Kouwenhoven, Studies in gas–solid fluidization, *Internal Report*, 1993, (Department of Chemical Engineering, University of Amsterdam).
14 K.V. Jacob and A.V. Weimer, High-pressure particulate expansion and minimum bubbling of fine carbon powders, *AIChEJ., 33* (1987) 1698–1706.
15 D.E. Hennephof, Influence of gas density on the stability of homogeneous flow in bubble columns, *Masters Thesis*, Department of Chemical Engineering, University of Amsterdam, 1993.
16 R. Krishna, J.W.A. de Swart, D.E. Hennephof, J. Ellenberger and H.C.J. Hoefsloot, Influence of increased gas density on hydrodynamics of bubble column reactors, *AIChEJ.*, in press.
17 M. Poletto, P. Salatino and L. Massimilla, Fluidization of solids with CO_2 at pressures ranging from ambient to nearly critical conditions, *Chem. Eng. Sci., 48* (1993) 617–621.
18 R. Krishna, P.M. Wilkinson and L.L. van Dierendonck, A model for gas holdup in bubble columns incorporating the influence of gas density on flow regime transitions, *Chem. Eng. Sci., 46* (1991) 2491–2496.
19 A. Biesheuvel and W.C.M. Gorissen, Void fraction disturbances in a uniform bubbly fluid, *Int. J. Multiphase Flow, 16* (1990) 211–231.
20 H.C.J. Hoefsloot and R. Krishna, Influence of gas density on the stability of homogeneous flow in bubble columns, *Ind. Eng. Chem. Res., 32* (1993) 747–750.
21 G.K. Batchelor, A new theory of the instability of a uniform fluidized bed, *J. Fluid Mech., 193* (1988) 75–110.
22 G.B. Wallis, *One Dimensional Two Phase Flow*, McGraw-Hill, New York, 1969.
23 J.M. Ham, S. Thomas, E. Guazzelli, G.M. Homsy and M.-C. Anselmet, An experimental study of the stability of liquid-fluidized beds, *Int. J. Multiphase Flow, 16* (1990) 171–185.
24 A. Schumpe and G. Grund, The gas disengagement technique for studying gas holdup structure in bubble columns, *Can. J. Chem. Eng., 64* (1986) 891–896.
25 G. Grund, Hydrodynamische Parameter und Stoffaustauscheigenschaften in Blasensäulen mit organischen Medien, *Ph.D. Dissertation*, University of Oldenburg, 1988.
26 A.W.M. Roes and C.N. Garnier, Investigation into the bubble-to-dense phase mass transfer rate in a gas–solid fluidized bed with cohesive powders, in W.P.M. van Swaaij and N.H. Afghan (eds.), *Heat and Mass Transfer in Fixed and Fluidized Beds*, Hemisphere, Washington, DC, 1986, p. 417.
27 H. Wezorke, Einfluss von Grossblasen in Blasensäulenreaktoren, *Ph.D. Dissertation*, University of Dortmund, 1986.
28 J. Werther, Problems of scaling up fluidized bed reactors, *Chem. Ing. Tech., 49* (1977) 777–785.
29 G. Grund, A. Schumpe and W.-D. Deckwer, Gas–liquid mass transfer in a bubble column with organic liquids, *Chem. Eng. Sci., 47* (1992) 3509–3516.
30 J.J. van Deemter, Mixing and contacting in gas–solid fluidized beds, *Chem. Eng. Sci., 13* (1961) 143.
31 R.C. Darton, R.D. LaNauze, J.F. Davidson and D. Harrison, Bubble growth due to coalescence in fluidized beds, *Trans. Inst. Chem. Eng., 55* (1977) 274–280.
32 R. Krishna, Design and scale-up of gas fluidized bed reactors, in A. Rodrigues, J.M. Calo and N.H. Sweed (eds.), *NATO Advanced Study Institute Series*, No. E52, *Multiphase Chemical Reactors*, Vol. II, *Design Methods*, Sijthoff and Noordhoff, Alphen aan den Rijn, 1981, p. 389.
33 R. Krishna, A unified approach to the design and scale-up of bubbling fluidized multiphase reactors, in B.D. Kulkarni, R.A. Mashelkar and M.M. Sharma (eds.), *Recent Trends in Chemical Reaction Engineering*, Vol. II, Wiley Eastern, New Delhi, 1987, pp. 234–264.
34 R. Krishna, Analogies in multiphase reactor hydrodynamics, In N.P. Cheremisinoff (ed.), *Encyclopedia of Fluid Mechanics*, Gulf, Houston, TX, 1993.
35 D.J. Vermeer and R. Krishna, Hydrodynamics and mass transfer in bubble columns operating in the churn-turbulent regime, *Ind. Eng. Chem. Process Design Develop., 20* (1981) 475–482.
36 N. Devanathan, D. Moslemian and M.P. Dudokovic, Flow mapping in bubble columns using CARPT, *Chem. Eng. Sci., 45* (1990) 2285–2291.
37 H.M.I. Baird and R.G. Rice, Axial dispersion in large unbaffled columns, *Chem. Eng. J., 9* (1975) 171–174.
38 Y. Kato, T. Fukuda and S. Tanaka, The behaviour of suspended solid particles and liquid in bubble columns, *J. Chem. Eng. Jpn., 5* (1972) 112–118.
39 A.S. Khare and J.B. Joshi, Effect of fine particles on gas hold-up in three phase sparged reactors, *Chem. Eng. J., 44* (1990) 11–25.
40 R.C. Darton, The physical behaviour of three-phase fluidized beds, in J.F. Davidson, R. Clift and D. Harrison (eds.), *Fluidization*, Academic, New York, 2nd edn., 1985, pp. 495–528.
41 H.I. de Lasa and S.L.P. Lee, Three-phase fluidized bed reactors, in H.I. de Lasa (ed.), *NATO Advanced Study Institutes Series*, No. 110, *Chemical Reactor Design and Technology*, Martinus Nijhoff, Dordrecht, 1986, pp. 349–391.
42 A. Gianetto, S. Pagliolico, G. Rovero and B. Ruggeri, Theoretical and practical aspects of circulating fluidized bed reactors (CFBRs) for complex chemical systems, *Chem. Eng. Sci., 45* (1990) 2219–2225.
43 J.R. Grace, High-velocity fluidized bed reactors, *Chem. Eng. Sci., 45* (1990) 1953–1966.
44 K. Schügerl, *Bioreaction Engineering*, Vol. 2, *Characteristic Features of Bioreactors*, Wiley, Chichester, 1991.

Appendix A: Nomenclature

a	interfacial area per unit expanded bed volume ($m^2\ m^{-3}$)
d	bubble diameter (m)
d_{large}	diameter of large bubbles (m)
d_p	mean particle size (m)
d^*	equilibrium bubble size (m)
D_{ax}	axial dispersion coefficient ($m^2\ s^{-1}$)
D_T	reactor diameter (m)
g	acceleration due to gravity, 9.81 $m\ s^{-2}$
h	height above gas distributor (m)
h_0	parameter determining initial bubble size at gas distributor (m)
h^*	height above gas distributor where bubbles reach their equilibrium size (m)
H	height of expanded bed (m)
H_0	height of ungassed bed (m)
k_{large}	mass transfer coefficient from dilute to dense phase ($m\ s^{-1}$)

n	Richardson–Zaki exponent
t	time (s)
U	superficial gas velocity (m s^{-1})
U_c	superficial velocity of continuous phase (m s^{-1})
U_d	superficial velocity of dispersed phase (m s^{-1})
U_{df}	superficial velocity of gas through dense phase (m s^{-1})
U_{mb}	minimum bubbling velocity for gas–solid fluid bed (m s^{-1})
U_{mf}	minimum fluidization velocity for gas–solid fluid bed (m s^{-1})
U_{trans}	superficial gas velocity at regime transition (m s^{-1})
v_∞	single-bubble rise velocity (m s^{-1})
V_{large}	rise velocity of large bubble population (m s^{-1})
V_{slip}	slip velocity between dispersed and continuous phases (m s^{-1})
V_{small}	rise velocity of small bubble population (m s^{-1})

Greek letters

ϵ	fractional holdup of gas bubbles
ϵ_c	continuous phase holdup
ϵ_d	dispersed phase holdup
ϵ_{large}	holdup of fast-rising large bubbles
ϵ_{mf}	voidage of fluidized bed at minimum fluidization
ϵ_{trans}	gas holdup at regime transition point
ϵ^{exp}	total bed expansion of gas–solid fluid bed
μ_L	liquid viscosity (Pa s)
ρ_G	density of gaseous phase (kg m^{-3})
ρ_L	liquid density (kg m^{-3})
ρ_p	particle density (kg_{cat} m^{-3})

Subscripts

c	continuous phase
d	dispersed phase
df	dense or emulsion phase
G	gas phase
l	large bubbles
large	large bubbles in gas–liquid systems
L	liquid phase
mb	minimum bubbling point
mf	minimum fluidization
p	particle phase
small	small bubbles in gas–liquid systems
trans	transition point
0	conditions at gas distributor ($h=0$)
∞	single particle or bubble

Superscripts

exp	expansion of fluid bed
*	equilibrium value